PHYSICAL REVIEW
LETTERS

VOLUME 18 | 26 JUNE 1967 | NUMBER 26

μ-ATOMIC LYMAN AND BALMER SERIES IN Ti, TiO_2, and Mn*

D. Kessler, H. L. Anderson, M. S. Dixit, H. J. Evans, and R. J. McKee
University of Chicago, Chicago, Illinois

and

C. K. Hargrove, R. D. Barton,† E. P. Hincks,‡ and J. D. McAndrew
National Research Council of Canada, Ottawa, Canada
(Received 17 May 1967)

μ-atomic Lyman and Balmer series were observed in Ti, TiO_2, and Mn using a large high-resolution Ge(Li) detector. While the relative line intensities are, for the most part, accounted for reasonably well by a cascade model, systematic differences were found in comparing the intensities in TiO_2 and Ti. The $2p$-$2s$ splitting was observed for the first time in muonic atoms.

The use of large high-resolution lithium-drifted germanium detectors[1] has made it possible to observe the spectral series in muonic atoms and to resolve clearly transitions from states with principal quantum number n as high as 7. In the present paper we describe intensity measurements made of the Lyman and Balmer series for titanium and manganese. These elements were chosen because the Lyman and Balmer lines lie in the interval 200 keV-2 MeV, where intensity measurements are most conveniently performed.

The germanium detector was a large-sensitive-volume (17 cm^3) coaxial diode[2] with a resolution better than 5-keV full width at half-maximum at 1 MeV. It was surrounded by a $2\frac{1}{4}$-in. thick NaI annulus (inner diameter $2\frac{3}{4}$ in., outer diameter $7\frac{1}{4}$ in., length 5 in.) viewed by four RCA 6292 photomultipliers. In addition to the spectrum of all Ge events (X spectrum) the spectrum of those events not vetoed by an NaI pulse ($X\bar{A}$ spectrum) was also recorded. In the $X\bar{A}$ spectrum the Compton continuum of the Ge detector is reduced. The muon telescope was similar to that of our previous work[3] except that two targets were used and stops in each target were labeled separately in the manner of Cohen et al.[4] Each germanium pulse following a muon stop was analyzed for pulse height and for time relative to the stop.[5] A PDP-8 computer recorded this information and, making use of the measured relation of time to pulse height for genuine prompt events, separated events into "prompt" (x-ray plus capture γ-ray) or "delayed" (capture γ-ray only) spectra. Both spectra were then stored separately in an ASI-6040 computer. The delayed spectrum was used to identify the capture γ rays and correct for their presence in the prompt spectrum. Electronic stabilization of the system minimized the drift and permitted the accumulation of data over long periods of time. An extended run was made in the case of Ti to show the spectral lines with good statistics and to allow fairly precise intensity measurements. The runs for manganese were of much shorter duration. Ti metal and TiO_2 spectra were recorded simultaneously to measure chem-

ical effects on the intensities as observed by Zinov et al.[6]

Figure 1 shows the muonic Lyman and Balmer x-ray series in Ti and Mn. We include in Fig. 1(e) a spectrum obtained with Fe as target showing the Paschen series as recorded in the $X\bar{A}$ mode. This spectrum is contaninated by carbon x rays produced by muon stops in the plastic scintillators. A capture γ ray identified by comparison with the delayed spectrum is indicated in Fig. 1(d).

Below each of the experimental spectra in Fig. 1 are plotted the spectral intensities calculated in the following manner. The x-ray intensities per stopped muon are obtained from cascade calculations similar to those by Eisenberg and Kessler.[7] Starting with a statistical population in the states with $n = 14$, the cascade is followed as it develops through Auger and radiative transitions until the ground state is

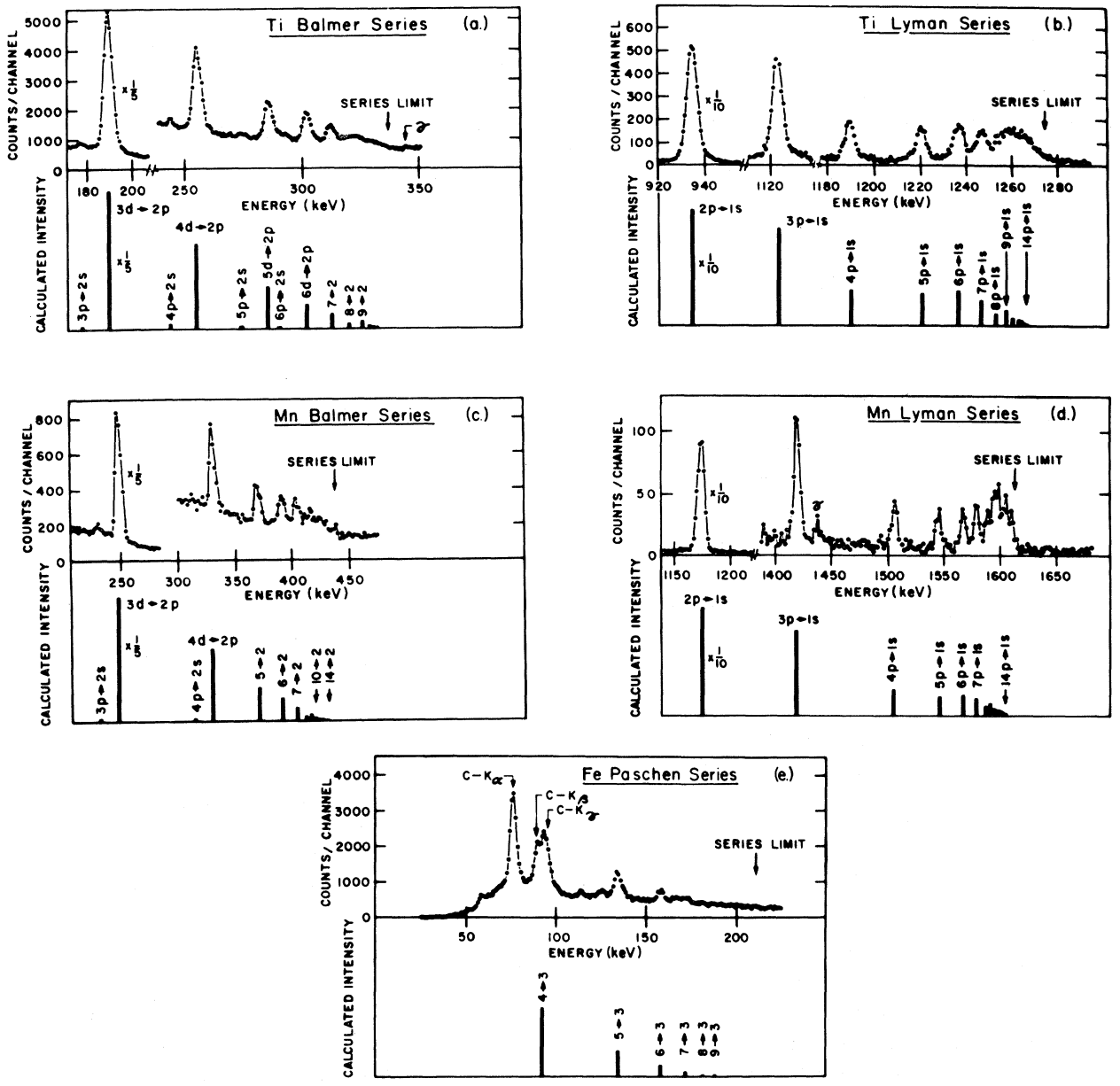

FIG. 1. Comparison of five experimental x-ray spectra with the predicted line spectra. The calculated intensities were derived from cascade calculations and corrected for target self-absorption and detector sensitivity. Channel widths: (a), (b) 0.8 keV; (c), (d) 1.6 keV; (e) 1 keV.

reached. By statistical population is meant a population proportional to $2l+1$ for a state of angular momentum l. We start the calculation at $n=14$, because at this value the muon Bohr orbit falls inside the electron K shell and electron shielding was neglected in the calculation. As mentioned in Ref. 7, the choice of an initial distribution in a particular level is less artificial than it would at first seem. This is due to the fact that the population distribution changes slowly as long as the Auger transitions, which favor small quantum jumps ($n \to n-1, l \to l \pm 1$), predominate over radiative transitions. For the elements under consideration here, this is true down to about $n=7$. The assumed initial distribution is therefore a characteristic of the whole group of higher levels and the results are not very sensitive to the starting value of n. To compare with the experimental spectra the calculated intensities were corrected for self-absorption in the target and for the energy dependence of the detector efficiency. The latter was determined experimentally with the help of the radioactive sources Gd^{153} and Ra^{226} using the standardizations outlined by Ewan and Tavendale.[1] The relative detector efficiency decreases by a factor of more than 20 between 200 keV and 2 MeV and we estimate that the relative efficiencies for lines widely separated in energy are good to about 25% only. However, as long as we consider only lines belonging to the same spectral series, systematic errors due to counter calibration are not very important.

The predicted spectra shown in Fig. 1 were normalized by making the calculated and measured α lines equal in amplitude. In the case of the Fe Paschen series, however, we normalized with respect to the M_β line because of the uncertainty in separating the M_α line from the carbon K lines in its vicinity. Only transitions of the type np-$1s$ contribute to the Lyman series. In the Balmer series the main contribution comes from the transitions nd-$2p$. These transitions and ns-$2p$, which are close in energy and contribute of the order of 1%, make up the main peaks of the Balmer series. The transitions np-$2s$, however, are lower in energy (by 11 ± 1 keV in Ti and 18 ± 1 KeV in Mn) and have an intensity which is a few percent of the main peak. They can be seen where the statistics are good enough and some of these secondary peaks are indicated in Fig. 1(a) and 1(c). The $2s$-$2p$ splitting, which is mainly due to the effect of the nuclear size, has been predicted by Wheeler[8] and, to our knowledge, is here reported for the first time. The measured shift agrees well with preliminary calculations and will be discussed in a forthcoming paper.

The qualitative agreement between the observed and calculated line strengths, as illustrated in Fig. 1, is remarkably good. In addition, there is little, if any, evidence for transitions from the continuum into one of the lower bound states.

A quantitative comparison between the predictions of the cascade calculation and the experimental results is shown in Table I. The experimental intensities were obtained by integration under the peaks in the X spectrum. The X spectrum, although it has higher background, was used because the x rays from the cascade can produce real coincidences between the Ge(Li) diode and the NaI annulus. These coincidences cause a loss of counts in the $X\bar{A}$ spectrum which can distort the relative intensities in a series by 10-15%. The data were corrected for self-absorption in the target and counter efficiency. The intensities were then normalized to the α line of each series. The quoted errors include the statistical errors and estimated uncertainties in the background subtraction and counter calibration. The K_β/K_α and K_ν/K_α ratios measured by Johnson, Hincks, and Anderson[9] and Quitmann et al.[10] are in substantial agreement with our values for these ratios.

In Table I the calculated relative intensities are given not only for a statistical initial distribution but for a more general distribution of the type

$$N(l) \propto (2l+1)\exp(al), \tag{1}$$

where a is an adjustable parameter. Positive a gives added weight to states with high angular momentum and negative a favors states with low angular momentum, as compared to statistical distribution.

Comparison of the calculations and the data for Ti shows that the resolved lines are in reasonably good agreement with the calculated values for $a=0$ and that values of $|a| \geq 0.1$ are unlikely as indicated by the χ^2's in Table I. However, the predicted intensity of the unresolved lines with $n \geq 8$ is too low by a factor of almost 2. The manganese data favor the predictions of the $a=-0.1$ calculation, although here again the unresolved higher lines are significantly

Table I. Comparison of measured intensities with calculated values.

	Transition	E (keV)	Experimental Intensities	Calculated intensities for a = -0.2	-0.1	0.0	+0.1	+0.2
$_{22}$Ti Lyman	2p-1s	942	1.000±0.005	1.000	1.000	1.000	1.000	1.000
	3p-1s	1122	0.102±0.003	0.146	0.122	0.102	0.083	0.068
	4p-1s	1189	0.031±0.004	0.065	0.051	0.039	0.029	0.022
	5p-1s	1220	0.036±0.003	0.069	0.051	0.037	0.025	0.017
	6p-1s	1236	0.041±0.003	0.085	0.058	0.039	0.025	0.015
	7p-1s	1246	0.023±0.004	0.072	0.046	0.029	0.017	0.009
	higher K	1253-1274	0.099±0.005	0.184	0.104	0.055	0.027	0.013
	χ^2 (higher K-lines excl.)			773.5	159.6	6.8	84.5	261.0
	χ^2 (higher K-lines incl.)			1021.3	160.4	73.2	262.2	514.6
$_{22}$Ti Balmer	3d,s-2p	190	1.000±0.006	1.000	1.000	1.000	1.000	1.000
	3p-2s	179	0.018±0.002	0.040	0.029	0.021	0.015	0.012
	4d,s-2p	255	0.180±0.006	0.268	0.230	0.196	0.166	0.142
	4p-2s	244	0.006±0.002	0.019	0.013	0.009	0.006	0.004
	5d,s-2p	286	0.099±0.012	0.189	0.147	0.112	0.084	0.063
	5p-2s	275	0.006±0.002	0.020	0.013	0.008	0.005	0.003
	6d,s-2p, 7p-2s	302, 301	0.081±0.007	0.175	0.119	0.079	0.052	0.034
	7d,s-2p, 8p-2s	312, 309	0.055±0.013	0.103	0.064	0.039	0.023	0.014
	higher L	319-340	0.102±0.033	0.210	0.112	0.057	0.028	0.014
	χ^2 (higher L-lines excl.)			677.7	170.1	15.3	32.7	116.4
	χ^2 (higher L-lines incl.)			688.4	170.2	17.2	37.8	123.5
$_{25}$Mn Lyman	2p-1s	1175	1.000±0.018	1.000	1.000	1.000	1.000	1.000
	3p-1s	1419	0.121±0.009	0.137	0.115	0.093	0.075	0.060
	4p-1s	1504	0.045±0.008	0.053	0.042	0.031	0.023	0.017
	5p-1s	1544	0.037±0.009	0.045	0.034	0.024	0.017	0.011
	6p-1s	1566	0.034±0.009	0.055	0.040	0.026	0.017	0.011
	higher K	1579-1613	0.191±0.015	0.245	0.145	0.080	0.042	0.021
	χ^2 (higher K-lines excl.)			10.4	1.1	15.6	42.2	73.1
	χ^2 (higher K-lines incl.)			23.4	10.5	70.4	140.9	201.5
$_{25}$Mn Balmer	3d,s-2p	247	1.000±0.032	1.000	1.000	1.000	1.000	1.000
	3p-2s	228	0.035±0.010	0.036	0.026	0.018	0.014	0.010
	4d,s-2p	330	0.164±0.015	0.239	0.204	0.173	0.146	0.124
	4p-2s	311	0.006±0.002	0.015	0.010	0.006	0.004	0.003
	5d,s-2p, 6p-2s	369, 372	0.121±0.029	0.163	0.126	0.095	0.071	0.053
	6d,s-2p, 7p-2s	391, 385	0.152±0.048	0.142	0.099	0.068	0.046	0.031
	higher L	404-438	0.317±0.056	0.331	0.188	0.104	0.057	0.031
	χ^2 (higher L-lines excl.)			47.4	13.2	14.7	14.7	27.5
	χ^2 (higher L-lines incl.)			47.5	18.5	29.2	36.3	53.5

more intense than the calculations give. The iron data are not presented in Table I because of their low statistical significance and problems introduced by the presence of capture γ rays and other contaminations.

We have obtained the following values for the L_α/K_α ratios in Ti and Mn: 0.52 ± 0.04 and 0.73 ± 0.06, respectively. The quoted errors refer to the statistics only. We expect, however, a large systematic error (of the order of 25%) due to detector calibration as the counter sensitivity changes by a factor of about 10 between the K and L lines. Differences in target self-absorption effects are also large for these lines. The calculated L_α/K_α ratios (for a statistical distribution at $n=14$) are 0.67 and 0.69, respectively.

The cascade calculations appear to be a useful tool in the understanding and interpretation of the x-ray series; however, the deviations are significant and suggest the need for a more sophisticated model. In general it appears that one cannot assume the same initial population in cascade calculations even for elements nearby in the periodic table. Low-Z elements require an initial distribution weighted for high-l states.[7] In the neighborhood of Ti ($Z=22$) a statistical distribution is required, while for higher Z a weighting of the low-l states gives a better fit to the data of Quitmann et al.[10] We have no explanation of this behavior at present.

The measurements of Zinov et al.[6] have shown that different compounds of the same element produce different relative intensities in the x-ray series. This observation is substantiated in the present work where the relative intensi-

Table II. Intensity ratios in titanium and titanium oxide.

	Ti	TiO_2	TiO_2/Ti
	Lyman series		
$\frac{3p-1s}{2p-1s}$	0.102 ± 0.003	0.093 ± 0.006	0.91 ± 0.06
$\frac{4p-1s}{2p-1s}$	0.031 ± 0.004	0.027 ± 0.005	0.87 ± 0.120
$\frac{5p-1s}{2p-1s}$	0.036 ± 0.003	0.025 ± 0.005	0.69 ± 0.14
$\frac{6p-1s}{2p-1s}$	0.041 ± 0.003	0.028 ± 0.005	0.68 ± 0.11
$\frac{\text{higher } K}{2p-1s}$	0.122 ± 0.007	0.062 ± 0.007	0.51 ± 0.06
	Balmer series		
$\frac{4d-2p}{3d-2p}$	0.180 ± 0.006	0.151 ± 0.006	0.84 ± 0.05
$\frac{5d-2p}{3d-2p}$	0.099 ± 0.003	0.073 ± 0.006	0.74 ± 0.07
$\frac{6d-2p}{3d-2p}$	0.081 ± 0.004	0.051 ± 0.006	0.63 ± 0.08
$\frac{\text{higher } L}{3d-2p}$	0.157 ± 0.009	0.078 ± 0.016	0.50 ± 0.11

ties of the Lyman and Balmer lines in TiO_2 are compared with those in Ti metal. Our results are given in Table II. These results show that the higher transitions in TiO_2 are systematically reduced compared to the same transitions in Ti. Moreover, the L_α/K_α ratio was found to be $(12 \pm 2)\%$ higher in TiO_2 than in Ti. Both results show that transitions between states of high l for given n are more favored in TiO_2 than in Ti. The origin of this "chemical" effect is not clear to us at present.

We wish to thank Frank Castorf, Rudy Gabriel, J. P. Legault, John Lillberg, William Miles, Paul Plowe, John Redfern, and Serena Torres for their contributions to the preparation and conduct of the experiment. We are grateful also to I. L. Fowler and H. L. Malm of Chalk River Nuclear Laboratories for the fabrication of the Ge detector and for helping to mount it.

---

*Research supported by the U. S. National Science Foundation and the National Research Council of Canada.

†Present address: Carleton University, Ottawa, Canada.

‡Also Carleton University, Ottawa, Canada.

[1]G. T. Ewan and A. J. Tavendale, Can. J. Phys. 42, 2286 (1964).

[2]Kindly loaned to us by Atomic Energy of Canada Limited, Chalk River Nuclear Laboratories.

[3]H. L. Anderson, C. S. Johnson, and E. P. Hincks, Phys. Rev. 130, 2468 (1963).

[4]R. C. Cohen, S. Devons, A. D. Kanaris, and C. Nissim-Sabat, Phys. Rev. 141, 48 (1966).

[5]R. D. Ehrlich, D. Fryberger, D. A. Jensen, C. Nissim-Sabat, R. J. Powers, B. A. Sherwood, and V. L. Telegdi, Phys. Letters 23, 468 (1966).

[6]V. G. Zinov, A. D. Konin, A. I. Mukhin, and P. V. Polyakova, private communication.

[7]Y. Eisenberg and D. Kessler, Nuovo Cimento 19, 1195 (1961).

[8]J. A. Wheeler, Rev. Mod. Phys. 21, 133 (1949).

[9]C. S. Johnson, E. P. Hincks, and H. L. Anderson, Phys. Rev. 125, 2102 (1962).

[10]D. Quitmann, R. Engfer, U. Hegel, P. Brix, G. Backenstoss, K. Goebel, and B. Stadler, Nucl. Phys. 51, 609 (1964).